



# Superplasticizer effects on setting and structuration mechanisms of ultrahigh-performance concrete

V. Morin<sup>a,\*</sup>, F. Cohen Tenoudji<sup>a</sup>, A. Feylessoufi<sup>b</sup>, P. Richard<sup>c</sup>

<sup>a</sup>Laboratoire Universitaire d'Application de la Physique (LUAP), Université Paris VII, 2, Place Jussieu, 75005 Paris, France

<sup>b</sup>Centre de Recherche sur la Matière Divisée (CRMD), CNRS and Université d'Orléans 45071 Orléans cedex, France

<sup>c</sup>Département de Génie Civil, Université de Sherbrooke, Sherbrooke, Quebec, Canada J1K 2R1

Received 20 October 1999; accepted 7 September 2000

## Abstract

The effect of superplasticizer addition on chemical and mechanical kinetics of ultrahigh-performance concrete realization is studied by ultrasonic spectroscopy, calorimetry, and autogenous shrinkage determination. Different percentages of superplasticizer have been used. We have firstly been able to identify the role of the superplasticizer on the early mechanisms of settlement of the solid particles in the mix, and the influence of entrapped air. The delay in the chemical activity brought by the superplasticizer has been analyzed according to the results of the three experimental methods. The continuous information upon the state of organization of the concrete and the structuration of the material is given by ultrasonics for any stage of the chemical reaction. A desynchronization of the shrinkage intense period versus the peak of released power and the material structuration is analyzed in terms of fissuration healing capability and material damaging. © 2001 Elsevier Science Ltd. All rights reserved.

**Keywords:** Superplasticizer; Concrete; Ultrasonics; Shrinkage; Setting

## 1. Introduction

Superplasticizers are playing an important role in the present development of ultrahigh-performance concrete. These new cement-based materials have a very low porosity, which is obtained by the addition in the formulation of very small reactive particles (diameter  $<0.5\ \mu\text{m}$ ) whose role is to fill the interstitial space between larger particles. This addition can lead to very dense, high-strength, hardened materials. Another positive point of this addition is that these new materials require a small amount of water because only a small quantity of hydrates is necessary to bind together the dense stack of solid particles. In fact, more hydrate formation obtained when using larger volumes of water could lead to materials of considerably lower strength.

When one mixes the dry particles with that small amount of water, the electric charges upon the solid particles tend to

cause their aggregation and prevent a good distribution of the water between solid particles, then preventing ultimately an optimal repartition of the hydrates formed between the particles. As such, the paste has a very low initial fluidity. Superplasticizer lowers the surface tension of water; its addition to the water is mandatory to allow the penetration of the fluid in between the solid particles and to give to these dense mixes an adequate permeability to water. A high level of fluidity can be maintained in spite of the low water content by the use of only small amounts of superplasticizers. One can then obtain a better pumping behavior for better shuttering or mold injection and a high-strength final concrete.

The kinetics of chemical mechanisms and the structural organization of particles and their cohesion are deeply influenced by superplasticizers even in small quantity. At the extreme, it is well known that beyond a critical amount of superplasticizer, the setting of concrete becomes impossible! In fact, the superplasticizer macromolecules modify the different forces maintaining the paste in its equilibrium: the repulsive electrostatic forces causing particle separation and the attractive hydrostatic capillary forces. These last forces are created by the air–water menisci

\* Corresponding author. LAFARGE Laboratoire Central de Recherche, 95 Rue du Montmurier, BP 15, 38291 Saint Quentin Fallavier cedex, France. Tel.: +33-4-7482-1824; fax: +33-4-7495-5623.

E-mail address: vincent.morin@pole-technologique.lafarge.com (V. Morin).

always present in a practical situation. The menisci induce a differential negative pressure in the interstitial medium and cause the cohesive forces within the mix. In the following, our interpretation of shrinkage mechanisms will be based on the forces balance in this three phases solid–liquid–gas medium.

In order to study the influence of superplasticizer in varying proportions on the rheology of the paste, its hardening, and the strength of the final concrete, we have developed a way of monitoring the particle organization and the mechanical properties based on two complementary mechanical and a chemical techniques: volumetric shrinkage, acoustic, and calorimetric measurements. This monitoring is used for the study of a formulation of ultrahigh-performance concrete. It brings insight on flow properties as well as on chemical and mechanical kinetic evolutions of the paste in the presence of superplasticizer addition.

## 2. Experimental

### 2.1. Material

The superplasticizer used is a copolymer of acrylic acid with acrylic ester [1] in water solution; it belongs to the last generation of macromolecules acting with a dual action: an anionic effect brought by a negative carboxylic ( $\text{COO}^-$ ) group and a volumetric steric effect given by the neutral oxyethylic branches. Its simplified chemical formula is given in Fig. 1, where the numbers of the different groups,  $n$ ,  $m$ , and  $p$ , are in the order of 17.

The ultrahigh-performance material used has the following components, particle size, proportion, expressed in

component to cement mass ratios (in parenthesis), respectively: Type V Portland cement, 20  $\mu\text{m}$  average diameter size (1); fine quartz sand, 310  $\mu\text{m}$  average diameter (1.1); silica fume, 0.2  $\mu\text{m}$  average diameter (0.25); water (0.21). In the present experiments, the superplasticizer is added to this formulation with three different dry extract to cement mass ratios (DE/C) of 0.5%, 1.1%, and 1.5%.

The dry concrete powder components are mixed for 3 to 5 min; water is added with half of the volume of the superplasticizer and mixed for 3 min, the remaining half of the volume of the superplasticizer is added and mixed for 5 min. This two-step procedure was adopted as it has been observed to give the best mixing results in these samples where the amount of water is overall small. The first addition humidifies the fine particles, which is favored by the mixing with a part of the superplasticizer; the second addition of the superplasticizer gives its fluidity to the mixture. The second introduction marks the start of time (hour 0). The mixture is degassed and immediately divided into two different samples: One sample is used for shrinkage determination, the second for acoustic and calorimetric experiments. No bleeding was observed, as the amount of water used in these high-performance concretes is very small.

### 2.2. Ultrasonic spectroscopy

An ultrasonic spectroscopic equipment is used to investigate the mechanical evolution of the setting and hardening of the concrete [2,3]. Both reflection and transmission of ultrasonic waves are studied. The technique uses short pulses of 1–2- $\mu\text{s}$  duration, which are analyzed in the time and in the frequency domain (after Fourier analysis of the ultrasonic pulses).

Broad-band longitudinal and shear wave transducers centered at 0.5 MHz are used. The mix is located in a Plexiglas cell shaped as a pillbox of 12-cm diameter and 2-cm height enclosed within 2-cm thick walls. Two pairs of transducers are fixed on the Plexiglas walls: one pair of longitudinal transducers facing each other, the other pair is used for shear waves. Four signals are analyzed: (a) the transmitted longitudinal signal after crossing the Plexiglas walls and the concrete; (b) the signal obtained from the reflection of the longitudinal wave by the first interface Plexiglas–cement; (c) and (d) the transmitted and reflected shear signals. The ultrasonic measurements cell is placed in a thermoregulated bath at 20°C. A thermocouple gives the temperature of the concrete within the cell; another thermocouple monitors the temperature of the bath.

The measurements are done every 5 min during 50 to 70 h. After completion of the experiment, a computer program performs the analysis of the several hundred of signals obtained; it extracts the reflection and transmission coefficients of the concrete as functions of frequency all along the setting and hardening. It gives also the velocities and amplitudes of the signals from which we can

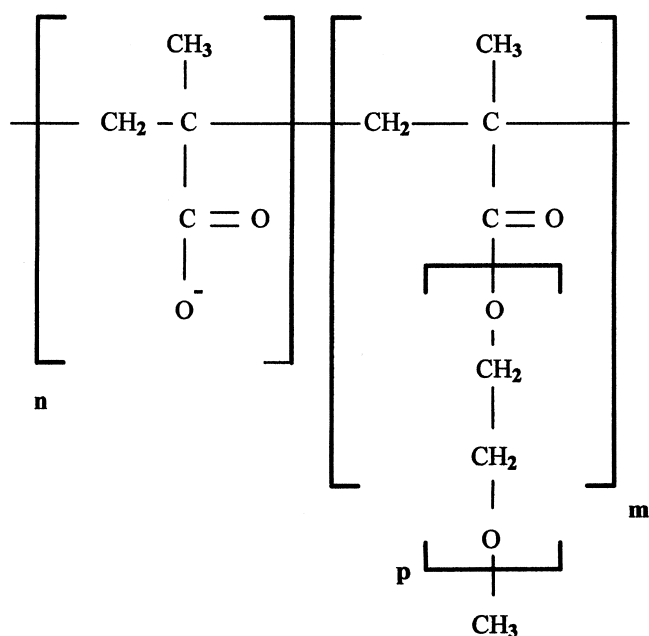


Fig. 1. Simplified chemical formula of the used superplasticizer molecule.

deduct the viscoelastic coefficients and the attenuations in the medium.

### 2.3. Autogenous shrinkage determination

As it will be discussed in the following, the volume of the paste will evolve all along the transformations of the paste. Two main reasons will be invoked: the particles' rearrangements under the internal interparticular forces and a chemical shrinkage due to the diminution of the molar volume during hydrates formation. Monitoring this volume variation (named autogenous shrinkage when the sample is isolated from external sources of water) will bring a lot of information about the transformations of the paste.

This autogenous shrinkage is obtained by an hydrostatic weight measurement procedure: Approximately 80 g of fresh concrete paste are sealed under vacuum in a thin rubber container just after mixing and weighed in water. The watertight rubber container follows the volume variations of the enclosed concrete. This sealed sample is placed in a water bath thermoregulated at 20°C within  $\pm 0.02^\circ\text{C}$  and its weight is measured by a scale with a precision of 1 mg. The scale is linked via a serial RS 232 link to a computer to calculate the volume variation inducing the Archimedean weight variation. Measurements are made every 30 s. This time interval corresponds to a relatively high measurement rate; it allows some redundancy in the sampling points used for decreasing the noise variances on the weight measurement and on its derivative versus time.

### 2.4. Calorimetry and hydration degree determination

Calorimetric measurements were made in order to calculate the hydration degree of the concrete specimen. The chemical reactions being exothermic, a sample with a large size would have its temperature increase strongly during the setting. In the method used here, one attempts to limit this temperature increase to 1–2.5°C at most by putting a sample of small size in an isothermal bath. This is the reason why this calorimetric method is called isothermal calorimetry. The released heat power is inferred from the small temperature difference  $\Delta T$  between the core of the sample and its exterior. The released power is then expressed by the addition of two terms: the first one is the product by the temperature difference  $\Delta T$  of the mean thermal conductance of the sample and of its container; the second term is proportional to the product of the mean calorific capacitance by the time derivative of the temperature difference,  $d(\Delta T)/dt$ . These two average parameter values are obtained after two calibration measurements. One can then calculate the heat power released by the chemical activity and, after time integration of that power, the released heat.

We note that  $Q$  is the measured heat produced at a given time and  $Q_{\text{infinite}}$  is the heat that would be produced in a complete hydration of cement. The value  $Q_{\text{infinite}}$  is calcu-

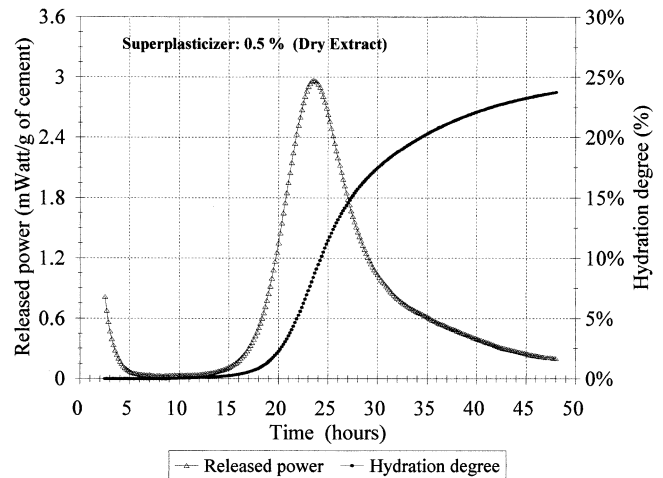


Fig. 2. Released power and hydration degree as a function of time.

lated from the enthalpies of the hydration reactions and the proportions of constituents. For the given concrete formulation,  $Q_{\text{infinite}}$  is estimated to be 483 J by gram of cement. The ratio  $Q/Q_{\text{infinite}}$  is noted alpha. This ratio is generally used as an expression of the hydration degree at a given time. The beginning ( $Q=0$ ) of the chemical reaction leading to hydrate formation is taken to be at the time where the temperature curves reaches its first minimum after the decrease in the first hours. In Fig. 2 are depicted the evolutions with time of the released power and the released heat for an amount of superplasticizer of 0.5%. Although alpha is an average indication for the whole set of exothermic reactions, this reactional parameter provides us with another basis of interpretation of aggregation and structuration mechanisms in parallel with the analysis versus time. We can then analyze the kinetic of evolution of the mechanical properties as given by ultrasonic spectroscopy and shrinkage measurements, either versus time or versus the amounts of reacted matter.

## 3. Results and discussion

In Fig. 3, we see the evolution of released heat power with time for three different samples with amounts of superplasticizer (DE/C of 0.5%, 1.1%, and 1.5%) from which alpha is calculated. The curves show a similar and typical evolution: An initial decrease of the power with the return of sample temperature toward bath temperature, followed by a dormant period. Then, the released power by the exothermic hydration reaction starts out to reach a maximum after several hours and then slows down. We may note immediately the delay brought in the chemical activity by the superplasticizer; this delay increasing with the amount of superplasticizer.

Let us now describe the chemical activity [4] and discuss the superplasticizer effect: During the first hours, the dicalcite and tricalcite silicate elements located on the cement

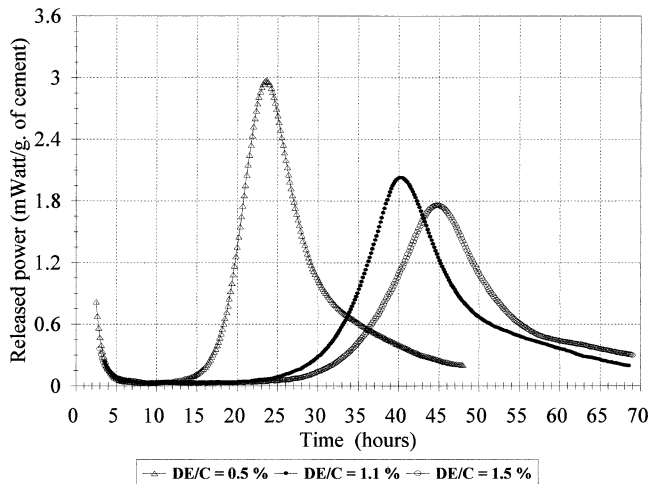


Fig. 3. Released power evolution with time for three amounts of superplasticizer dry extract (DE/C = 0.5%, 1.1%, and 1.5%).

grains surface dissolve partially and release calcium, hydroxyl, and silicate ions that combine to form calcium silicate hydrates (CSH) in exothermic reactions. This is the cause of the initial heat release observed at the beginning of the curves. As a consequence of the nonstoichiometry of the solution versus the hydrate formation, these reactions leave free unreacted hydroxyl and calcium ions. This induces a steep increase of the pH toward 12.8 that causes a slow down of the silicates dissolution rate and of the subsequent ions recombination in hydrates formation. During this dormant period of several hours where very low released heat is measured, the calcium ions concentration increases steadily. When a saturation level in calcium ions is reached, portlandite precipitates, the concentration in calcium and hydroxyl ions drops, the pH decreases, and the dissolution of silicate on grains surface may restart to lead to the formation of CSH that are mainly located upon grain surfaces. A new start of the released heat is observed. The chemical activity becomes intense. However, the diffusion of dissolved ions through the CSH hydrates layers is going to be more and more hindered by the amount of hydrates formed. As a consequence, the power released will decrease after having reached a maximum.

By comparison of the three curves in Fig. 3, we have already noticed the important delay on the chemical activity brought by a large amount of superplasticizer and we can note also that the released heat power peak at the period of maximum activity reached is more important for lesser amounts of superplasticizer. This slowing down of the chemical activity brought by the superplasticizer may be explained by the following argument: Before the addition of water, the cement grains carry surface charges created during the milling process. Within the solution, the polar head of the superplasticizer macromolecules fixes itself upon the surface and causes a slow down of the kinetics by impeding the ions diffusion starting from the grains and then hampers the hydrates formation. It has been found that

the hydration degree corresponding to the maximum temperature reached is the same, of the order of 9% in all cases. It appears that the volume of hydrates reached at this point is clearly related to the beginning of the decrease in reactivity of the mix.

In Fig. 4 is presented as function of time, the volumetric shrinkage  $\Delta V/V_0$  for the three superplasticizer amounts. The initial volume,  $V_0$ , just after mixing is estimated by a polynomial extrapolation of the volume variation toward  $t=0$ , as the time needed for the preparation of the sample (1 h) does not allow measurements at first instants. It is apparent that at any time, the shrinkage increases with the amount of superplasticizer. The shrinkage rate is large at the beginning and decreases with time in a first period. All samples present a restart of shrinkage occurring at 20 h for 0.5%, 45 h for 1.1%, and 50 h for 1.5%.

The representation of shrinkage as a function of the hydration degree gives more insight on the relations between the mechanical and the chemical aspects of the problem. In Fig. 5, the volumetric shrinkage is presented versus  $\alpha$  for the three superplasticizer ratios. We observe that after a quick rise, the curves reach a plateau followed by a second rise. The important increase of shrinkage at the beginning occurs before the dormant period, i.e., before a significant hydration degree ( $\alpha < 0.5\%$ ). So, this first shrinkage should be attributed to early settlement mechanisms of the material unrelated to the advancement of the chemical reaction. As it was noticed before in the analysis versus time, we see that the plateau level increases with the amount of superplasticizer. These differences in curves versus  $\alpha$  show that the superplasticizer plays a dominant role not only in slowing down the chemical kinetics but in mechanisms responsible of the early shrinkage too.

Let us look how the superplasticizer molecules that are adsorbed upon the solid particles provoke their deflocculation and are responsible of the dynamic rearrangement and how the shrinkage is induced as a consequence. The

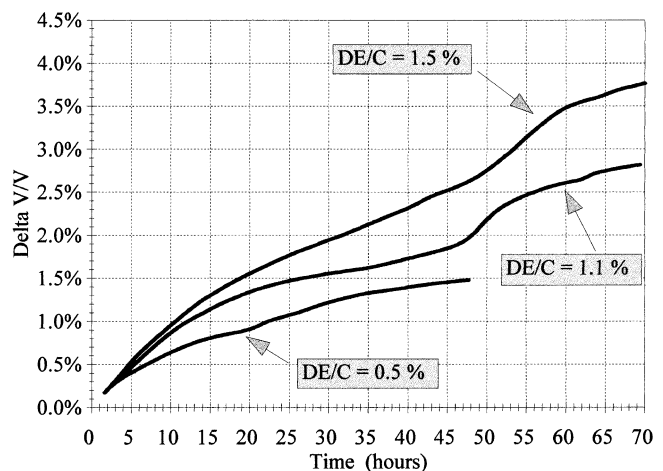


Fig. 4. Volumetric shrinkage for different superplasticizer amounts as functions of time (DE/C = 0.5%, 1.1%, and 1.5%).

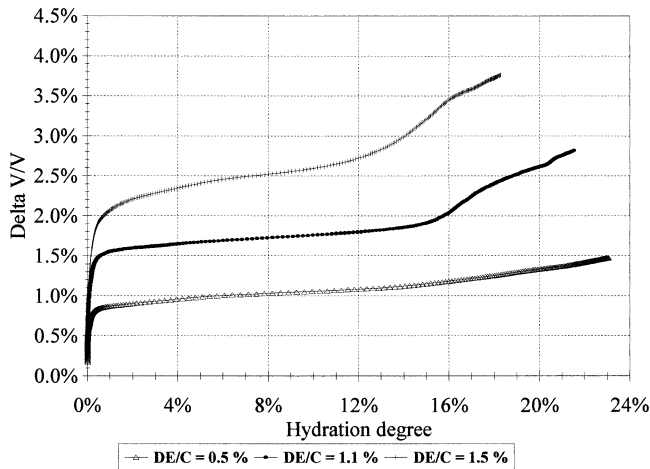


Fig. 5. Volumetric shrinkage for different superplasticizer amounts as functions of  $\alpha$ .

description generally admitted to describe these phenomena, which we share is the following [4]: as was said before, static charges exist at the particles surfaces before mixing with water; the positive charges can be partly compensated by free electrons of the atmosphere but the negative ones may remain unbalanced. In the absence of superplasticizer, in the ionic solution resulting of the partial silicates surface dissolution, these negative charges may be screened by a layer of positive ions (calcium) that create the so-called ionic double layer. When the particle distance is greater than the layer thickness, the electrostatic screening is total; a complex solid particle appears neutral to its neighboring particles. It appears that these neutral complexes have a tendency to coagulate mainly under the action of the attractive capillary forces, the repulsive electrostatic forces having vanished. As a consequence, the paste has a very low fluidity.

In presence of superplasticizer, the fixation of the large superplasticizer molecules upon the surface provokes an enlargement of the screening layer by diminishing the positive ion concentration in the vicinity of the negatively charged solid particles. The range of repulsive forces between particles is increased. At large, interparticular, distances, the electrostatic repulsive forces remain and are able to keep the particles apart. On the other hand, for a constant meniscus radius, the cohesive force induced by capillarity diminishes when the surface tension is lowered by superplasticizer.

As a consequence, the paste gains in fluidity and particles rearrangements are made possible. This effect has firstly been shown by Daimon and Roy [5] who evaluated the  $\zeta$  surface potential in cement mixes and showed how the flowing ability increases with the superplasticizer amount.

The second important effect of the addition of superplasticizer is that it favors air entrapment and microbubbles formation during the mixing by lowering the surface tension

of the interstitial fluid. This can be explained by the following argument: for a given energy of mixing determined by a given mixing duration, a lower surface tension will lead to a larger air–liquid surface contact expressed in the form of a greater number of bubbles and/or a lower bubbles radii. In consequence, after mixing, the degassing process will be less effective in the formula containing a larger amount of superplasticizer, as the smaller bubbles met in these samples are more effectively trapped in the interstices. Then, the remaining volume air fraction after degassing will be larger in samples having larger superplasticizer amounts. This effect is observable on the initial densities of the three compositions, which were estimated, respectively, to be 2.100, 2.072, and 2.070 for superplasticizer fractions of 0.5%, 1.1%, and 1.5%.

The shrinkage forces will be provided by the negative pressure in the interstitial fluid provoked by the air–liquid menisci. Again, an increased amount of superplasticizer will favor greater shrinkage as caused by the larger volume of entrained air and by the depression brought by the smaller menisci radii of the small bubbles met in that situation. Under the effect of these pressure forces, the solid particles will tend to reassemble and then squeeze the air–vapor bubbles volume.

In the beginning, the shrinkage is important because the capillary forces are dominant (when the volume of air is large). Furthermore, the shrinkage remains noticeable for an extensive period of time during the dormant period. This may be related to the fact that during that period, the calcium positive ions concentration increases continuously. In spite of the superplasticizer molecules present, these ions will progressively increase the screening of the negative charges on the solid particles surface [5–7] and, in consequence, diminish gradually the repulsive forces between the complex solid particles. The shrinkage will continue (with a decreasing rate) as long as the double layer thickness is important and the porous space offers room. When the calcium ions concentration reaches a saturation level, calcium hydrate (portlandite) products start to be formed in important amounts in the mix and favors a rapid formation of CSH in an exothermic reaction. This stage is considered as the end of the dormant period; the heat released begins to be significative and now increases rapidly with time. At this stage, one may consider that the shrinkage had been only caused by the capillary forces. As seen on the representation shrinkage versus  $\alpha$  in Fig. 5, the leveling of each curve marks the end of this first period of intense shrinkage with none or low  $\alpha$ . The level of the plateau appears to be grossly proportional to the superplasticizer fraction. In fact, for the amounts of 0.5%, 1.1%, and 1.5%, it has been observed that this rate is, respectively, 0.5%, 1%, and 1.3% at the beginning of the hydration reaction. The reason is that more superplasticizer induces more air-entrapping for a given mixing procedure and then, as discussed before, greater shrinkage capabilities. In summary, a certain amount of air grossly proportional to the quantity of superplasticizer

is entrained during the mixing and progressively dissolves in the water during the settling period.

These conclusions on the behavior within the first period can be completed by the information brought by the acoustical measurements.

In Fig. 6a is presented the evolution of the longitudinal Plexiglas–concrete reflection coefficient measured in echographic mode at 600 kHz as functions of time for the three superplasticizer additions. The three initial values are significantly different, the lesser adjuvanted formula (0.5%) has the lowest reflection coefficient; this means that the longitudinal acoustic impedance has a value nearer that of Plexiglas. For the higher superplasticizer amounts, the reflection coefficient is higher. The corresponding lower impedances express the fact that the elastic coupling between particles is more compliant for larger amounts of superplasticizer. This confirms the presence of entrapped air between the particles. We note that the higher reflection coefficient corresponds to the intermediate value of superplasticizer. This is not surprising, as it has been observed [1]

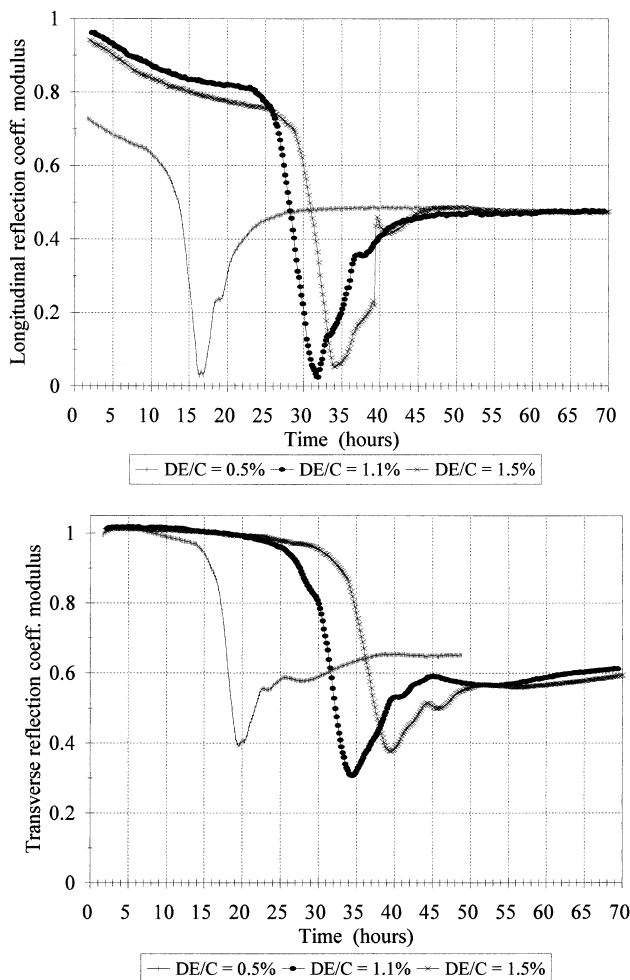


Fig. 6. Evolutions of the longitudinal (a) and transverse (b) acoustical reflection coefficient (at 600 kHz) with time for different amounts of superplasticizer (DE/C=0.5%, 1.1%, and 1.5%).

by classical torque–viscometer rheological measurements that an optimal low viscosity was obtained for an intermediate  $\approx 0.8\%$  superplasticizer addition for the same material formulation. We also observed a decrease of the longitudinal reflection coefficient during the first hours after mixing. It is important to recall that the chemical activity has not started yet and that this effect must correspond to the settlement of the paste, already described for the early age shrinkage phase.

On the contrary, the reflection coefficient of transverse waves is not sensitive to the amount of air, the initial values for the three superplasticizer amounts being very similar, nearly equal to 1 (Fig. 6b). The transverse acoustic impedance of the three pastes is very low.

Then, although longitudinal waves could be transmitted by mere solid contacts between the particles, these contacts are strongly affected by the air entrained by superplasticizer, which explains the strong dependence of longitudinal reflection coefficient. No bounds exist between the solid particles, preventing the elastic coupling of the shear displacements causing the independence of transverse reflection coefficient.

We may conclude from the later discussion that the Plexiglas–concrete reflection coefficient of longitudinal waves is very sensitive for detecting the presence of entrapped air and evaluating its amount.

We observe in a second phase a strong decrease of both longitudinal and transverse reflection coefficients for the three adjuvantations. These strong decreases of the reflection coefficient observed (beginning at hours 10, 25, and 30 for, respectively, superplasticizer DE/C ratios of 0.5%, 1.1%, and 1.5%) correspond to the rapid increase of the elastic moduli caused by the progressive binding of solid particles by hydrates. A reflection coefficient reaches its minimum when the acoustic impedance of the paste tends to that of the Plexiglas. Passed this minimum, as the impedances keep growing, the reflection coefficients increase again.

Using alpha as the variable in Fig. 7a,b,c, we observe for the three adjuvantations, when alpha is between 1% and 4%, a dispersion of the transverse reflection coefficient curves at three different frequencies showing as bundles. This dispersion is caused by the sensitivity of the different acoustic wavelengths to the connected clusters whose sizes vary with the hydration degree. For an alpha of approximately 1%, we note a sharp decrease of the reflection coefficients, the reflection coefficient decreasing more abruptly for the lower frequency. During this period, the medium has similar wave propagating frequency characteristics to those of a mass-spring chain.

At alpha=3.5%, the bundle of the reflection coefficients curves has converged. At this hydration degree, the material reaches its complete hyperstatic configuration [8], no degree of freedom remaining for any particle.

We will analyze this behavior in Fig. 8a,b,c depicting the time derivative (with sign changed) of the volume shrinkage

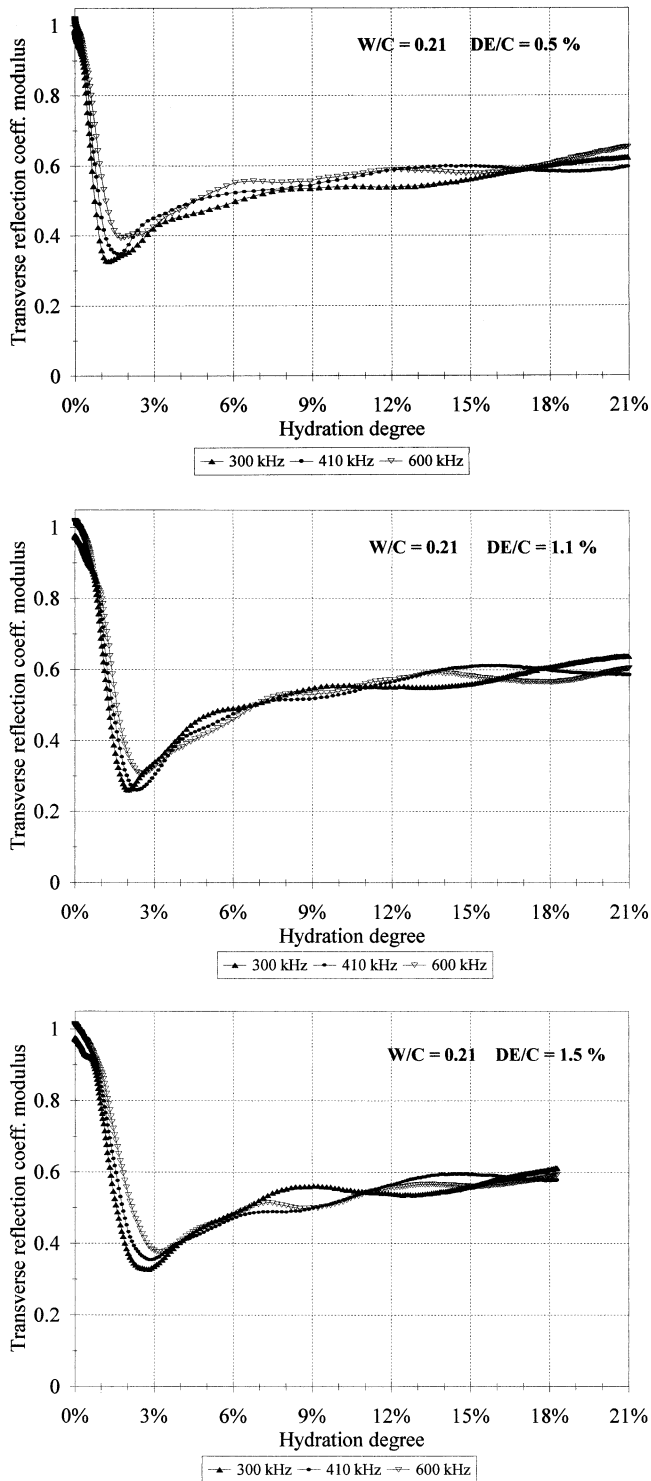


Fig. 7. Evolutions of the transverse acoustical reflection coefficient at three selected frequencies (300, 410, and 600 kHz) versus  $\alpha$  for different amounts of superplasticizer: (a)  $DE/C = 0.5\%$ ; (b)  $DE/C = 1.1\%$ ; (c)  $DE/C = 1.5\%$ .

and the released power for the three adjuvanted formula as functions of time.

We observe after the initial period of particles settlement appearing as a continuous decrease of the shrinkage rate, a

reincrease of the rate corresponding to the start of the thermal peak. The first maximum of the rate is reached at hours 21, 36, and 41, respectively, for  $DE/C$  of 0.5%, 1.1%, and 1.5%. These three hours correspond for all the samples to the same hydration degree  $\alpha = 3.5\%$  where, simulta-

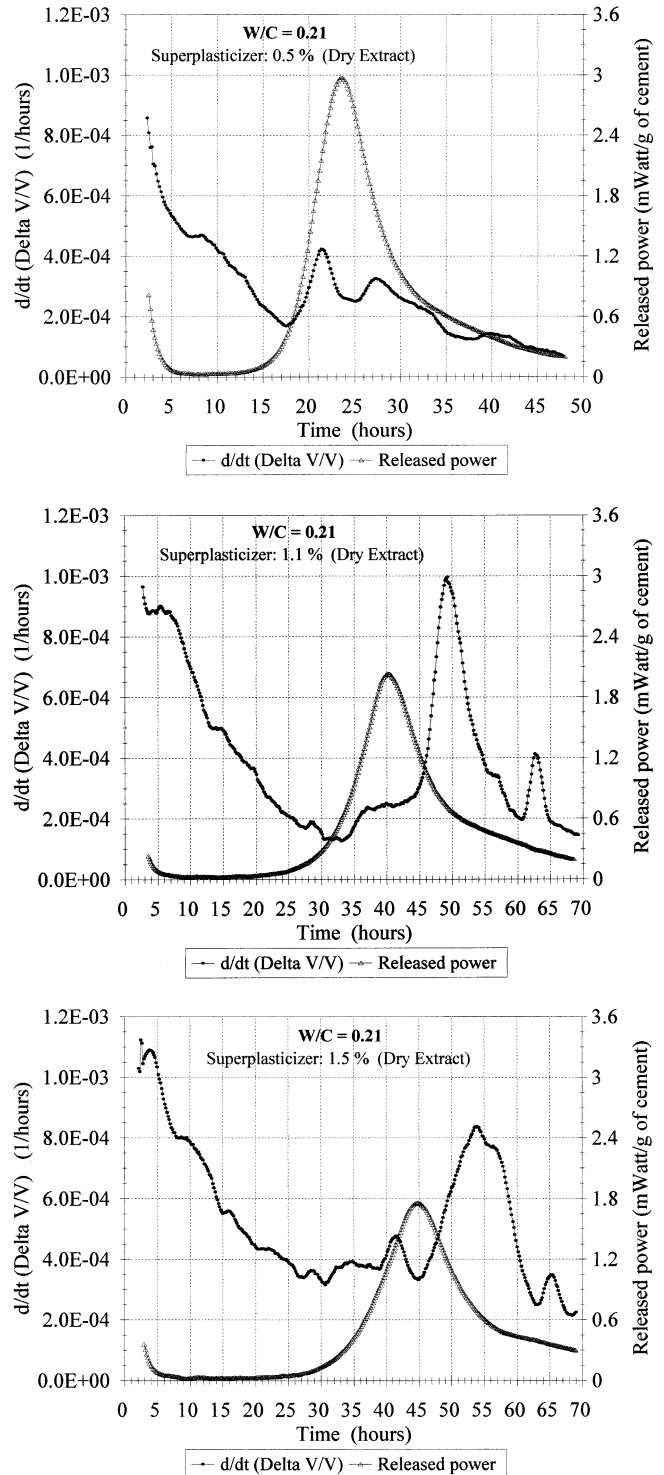


Fig. 8. Volumetric shrinkage time derivatives and released power evolutions versus time for three amounts of superplasticizer: (a)  $DE/C = 0.5\%$ ; (b)  $DE/C = 1.1\%$ ; (c)  $DE/C = 1.5\%$ .

neously, the reflection coefficient curves reach the end of the dispersive period (Fig. 7a,b,c). For this value of  $\alpha$ , the medium reaches its fully connected locked frame state; the shrinkage begins to be impeached and its rate slows down. For the three adjuvantations, the shrinkage rate reincreases at the maximum of the thermal peak. A priori, this last fact may appear paradoxical, as the shrinkage should be decreasing if it were directly related to the diminishing production of hydrates at this stage. A direct relationship would imply that a diminution of volume is directly tied to the formation of hydrates that have higher density than the average density of initial constituents, silicates, and water. We should emphasize also that for our formulations of reactive powder concrete (RPC), the maximal released power occurs at  $\alpha = 8.5\%$ . Although in concretes without fine particles and then with a higher porosity, it occurs for  $\alpha$  in the order of 15%. Our interpretation of this difference is that the beginning of the decrease of the thermal activity is caused in RPC by the progressive closure of capillary porosity [9], which at this stage hampers the ionic diffusion. It then seems apparent to us that the much smaller pores in RPC play a role in the chemical kinetics. The average pore radius will be diminishing and then, the capillary shrinkage forces inversely proportional to pore radius will increase. It is noted that the volume dilatation due to elevation of temperature is quite negligible because the measured amplitude of temperature variation in the core of the sample is less than  $0.5^\circ\text{C}$ , the sample being located in a thermostated bath.

For the two more adjuvanted formulas (Fig. 8b,c), a phase of intense shrinkage occurs after the thermal peak. This shrinkage will be necessarily accompanied by microfissuration in the material, which at this stage is fully structurally framed. This delay of the shrinkage peak versus the thermal activity seems to be damaging for the integrity of the material, which at this stage lacks the ability of self-healing, the intense hydrates formation period (thermal peak) being passed.

In Fig. 9, we represent the evolution with  $\alpha$  of the derivative of shrinkage versus  $\alpha$  for the three amounts of superplasticizer. It is interesting to compare the amplitude of this derivative to the volume diminution calculated from the chemical equation reaction. The total hydration reaction of pure tricalcic silicate  $\text{C}_3\text{S}$  (that mainly presents the same behavior as the cement), is accompanied by a molar volume diminution of 10% [10]. When taking into account the volume proportions of sand and silica fume present in our samples, the global volume diminution should be 0.05% by percent of  $\alpha$ . As seen in Fig. 9, after the high initial rate due to particles settling, the rate levels to a value in the order of the chemical shrinkage rate until  $\alpha = 3.5\%$ . As said earlier, for  $\alpha = 3.5\%$ , the shrinkage is impeached by the particle connection and decreases to values inferior to 0.05% that is the chemical shrinkage rate. The rate will stay inferior to 0.05% in the less adjuvanted formula ( $\text{DE/C} = 0.5\%$ ) but will increase strongly above this value for the two high adjuvantations

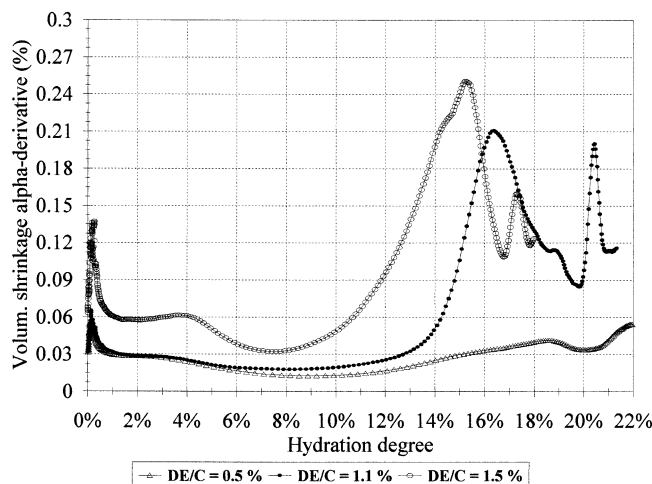


Fig. 9. Volumetric shrinkage  $\alpha$  derivatives versus  $\alpha$  for three amounts of superplasticizer ( $\text{DE/C} = 0.5\%$ ,  $1.1\%$ , and  $1.5\%$ ).

( $\text{DE/C} = 1.1\%$  and  $1.5\%$ ). We believe that, for the two latter adjuvantations, strong microfissuration occurs, because the material is fully framed but does not still possess its full strength. This microfissuration occurring for high values of  $\alpha$  and less quantities of hydrates still to be formed, the material has low healing capabilities.

In that respect, the formulation with  $\text{DE/C} = 0.5\%$  that has a flat shrinkage rate versus  $\alpha$  presents a better guarantee of higher strength. Properly, for this concrete formulation, this value of adjuvantation has been proven [11] to be optimal for its better compressive strength.

#### 4. Conclusion

We have studied the effect of the dosage of superplasticizer upon the evolution of the mechanical behavior of RPC using an analysis combining three techniques.

We have demonstrated the following effects:

- An important induced delay in the thermal activity increasing grossly proportionally to the adjuvantation and a released peak power decreasing within that proportion. The different relations between the structuration of the material and the chemical activity have been demonstrated by acoustics. In particular, the degree of hydration corresponding to the completion of the rigid frame and the temperance of the chemical activity accompanying the pore closure.
- A higher value of the acoustical reflection coefficient for the intermediate adjuvantation ( $1.1\%$ ) concurring with the fact that the rheological optimum lies in its vicinity ( $\approx 0.8\%$ ).
- An initial shrinkage increasing with the amount of adjuvantation occurring before the main chemical reaction. This shrinkage partly compensates the volume augmentation during mixing caused by the air entrapment induced by the superplasticizer.



- A later shrinkage occurring long after the peak released power, where, as shown by acoustics, the material has found its final structural state. At this stage, the material is susceptible to fissuration and has small healing capabilities, the main active hydrate formation period being passed. This shrinkage appears as a greater problem in the two more adjuvanted formula where the shrinkage is the more intense.

The beneficial effect on the rheological properties may be unfavorably balanced by the later period of intense shrinkage observed in the highly adjuvanted formula that can cause unhealed fissuration.

So, for a given application, an optimum superplasticizer amount should be looked for under the constraints brought by the aims of flowing capabilities before setting and by the necessity of ultimate strength.

### Acknowledgments

The authors would like to thank C. Vernet and J. Dugat from Bouygues for very stimulating discussions and precious information upon the material.

### References

- [1] O. Bonneau, C. Vernet, M. Moranville, Optimization of the rheological behavior of reactive powder concretes (RPC), Proc. Int. Symp. High Perform. Concr. React. Powder Concr. 3, Sherbrooke University Ed., Sherbrooke, 1998, pp. 99–118.
- [2] V. Morin, F. Cohen Tenoudji, C. Vernet, Study of the viscoelastic behavior of cement pastes at early ages with ultrasonic waves in echographic mode, Proc. Second RILEM Workshop Hydration Setting, Dijon 1997.
- [3] V. Morin, F. Cohen Tenoudji, C. Vernet, A. Feylessoufi, P. Richard, Ultrasonic spectroscopy investigation of the structural and mechanical evolutions of reactive powder concretes, Proc. Int. Symp. High Perform. Concr. React. Powder Concr. 3, Sherbrooke University Ed., Sherbrooke, 1998, pp. 119–126.
- [4] C. Vernet, Chimie des ciments, in: J. Baron, J.P. Ollivier (Eds.), La Durabilité des Bétons, Presses de l'Ecole Nationale des Ponts et Chaussées, Paris, 1992, pp. 100–106.
- [5] M. Daimon, D.M. Roy, Rheological properties of cement mixes: zeta potential and preliminary viscosity studies, Cem. Concr. Res. 8 (6) (1978) 753–764.
- [6] E. Nägele, The zeta potential of cement, Cem. Concr. Res. 15 (3) (1985) 453–462.
- [7] L. Nachbaur, P.C. Nkinamubanzi, A. Nonat, J.C. Mutin, Electrokinetic properties of CSH; Relation with coagulation process, Proc. Second RILEM Workshop Hydration Setting, Dijon.
- [8] A. Feylessoufi, F. Cohen Tenoudji, V. Morin, Early ages shrinkage mechanisms of an ultra high performance cement based material, Cem. Concr. Res., submitted for publication.
- [9] V. Morin, F. Cohen Tenoudji, A. Feylessoufi, P. Richard, Evolution of the capillary network in a reactive powder concrete during hydration process, Cem. Concr. Res., submitted for publication.
- [10] A. Boumiz, C. Vernet, F. Cohen Tenoudji, Mechanical properties of cement pastes and mortars at early ages, Adv. Cem. Based Mater. 3 (3–4) (1996) 94–106.
- [11] J. Dugat, private communication.